NANO LETTERS

LETTER

pubs.acs.org/NanoLett

Optical Nanorod Antennas Modeled as Cavities for Dipolar Emitters: Evolution of Sub- and Super-Radiant Modes

Tim H. Taminiau,*[,†] Fernando D. Stefani,[‡] and Niek F. van Hulst*[,†,§]

[†]ICFO-Institut de Ciencies Fotoniques, Mediterranean Technology Park, 08860 Castelldefels (Barcelona), Spain

[‡]Departamento de Física & Instituto de Física de Buenos Aires (IFIBA, CONICET), Universidad de Buenos Aires, Pab. I Ciudad Universitaria, 1428 Buenos Aires, Argentina

[§]ICREA-Institució Catalana de Recerca i Estudis Avançats, 08015 Barcelona, Spain

Supporting Information

ABSTRACT: Optical antennas link objects to light. Here we derive an analytical model for the interaction of dipolar transitions with radiation through nanorod antenna modes, by modeling nanorods as cavities. The model includes radiation damping, accurately describes the complete emission process, and is summarized in a phase-matching equation. We analytically discuss the quantitative evolution of antenna modes, in particular the gradual emergence of subradiant, super-radiant, and dark modes, as antennas become increasingly more bound, i.e., plasmonic. Our description is valid for the interaction of nanorods with light in general and is thus widely applicable.

KEYWORDS: Optical antennas, nanoantennas, metal nanorods, subradiance, dark modes, electric and magnetic dipole emitters

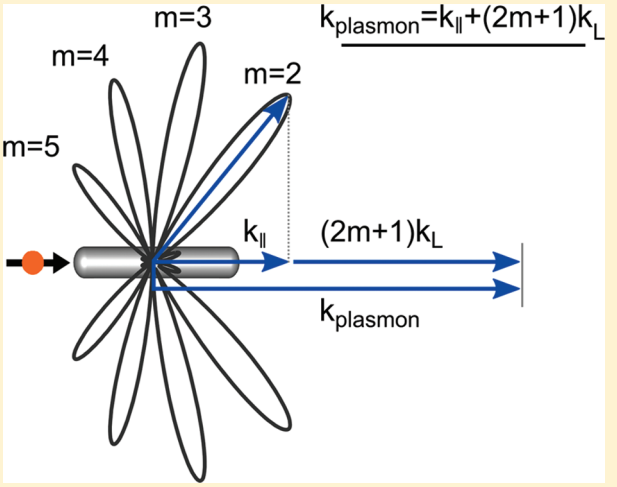

Optical antennas improve the interaction of an object with optical radiation by means of a near-field coupling. The object absorbs and emits light through the antenna modes.[1,2] Metallic nanoparticles are especially suited as optical antennas because they support confined plasmon modes that respond strongly to light.[3,4] With optical antennas, the electronic transitions of quantum emitters, such as molecules and quantum dots, can be controlled. Excitation and emission rates are enhanced,[5−7] the spectral dependence shaped,[8] and the angular emission directed.[2,9,10]

To understand optical antennas, and how they differ from conventional antennas, the Mie solutions are available for ellipsoids[8,11] and extensive numerical studies are performed for other shapes.[12] More intuitively, antennas have been described as resonators or (Fabry−Pérot) cavities.[1,13−22] If the wave vector along the antenna is known, the spectral position of the resonant modes can be determined.[23−25] However, the functionality of an antenna is not given by the value of the resonance length or wavelength alone, but by how its modes interact with a local object and with radiation.

In this Letter, we derive an analytical model for the interaction of dipolar transitions with radiation through nanorod optical antenna modes, by treating nanorods as one-dimensional cavities. The wavelength in the cavity is given by the waveguide modes of an infinitely long rod, whereas the reflection coefficient at the antenna ends is determined by the radiation damping of the formed cavity mode. The obtained analytical model accurately describes all the emission characteristics: the radiative decay rate, quantum efficiency, and angular emission. We use the model to quantitatively reveal the continuous evolution of antenna modes from perfectly conducting antenna theory to quasi-static plasmonics, i.e., from macroscopic to nanoscale antennas, with a focus on the gradual emergence of super-radiant, subradiant, and dark modes.

Consider an elongated antenna of physical length L_p with a central section, of constant cross-sectional shape and size, that supports a charge density wave with wave vector $\mathbf{k} = k\hat{\mathbf{z}}$

$$k = k' + ik'' \tag{1}$$

The wave is reflected at both the antenna ends, which form a resonator that we model as a two-mirror cavity, Figure 1a. The model developed applies to any cross-sectional shape, provided that k can be determined.

The waves originate from a local source at position $z = a$ along the antenna axis. Figure 1 shows three different sources: an electric dipole, a magnetic dipole, and a transmission line. The

Received: October 31, 2010
Revised: January 28, 2011

   dx.doi.org/10.1021/nl103828n | *Nano Lett.* XXXX, XXX, 000–000

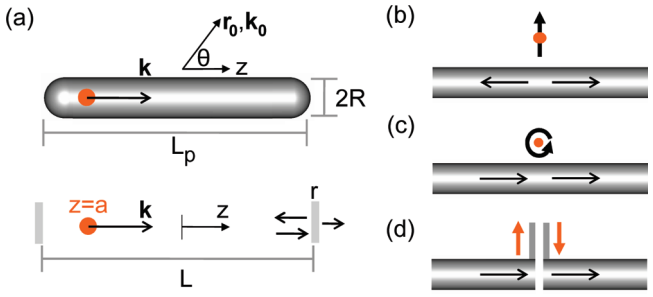

Figure 1. (a) The antenna (total length L_p) is a rod of constant cross-sectional shape and size that supports a charge-density wave (wave vector **k**), which is reflected at both antenna ends. We model the antenna as a 1D cavity with length L and amplitude reflection coefficient r. The antenna is driven by a local source at position $z = a$. As a concrete example to compare to numerical calculations, we study gold cylindrical antennas with radius R and hemispherical ends. (b−d) Three local sources and the direction of the waves induced: (b) electric and (c) magnetic dipole, (d) transmission line.

dipoles represent electronic dipolar transitions, such as those in a single molecule or quantum dot; transition rates are proportional to the emitted power. Electric and magnetic dipoles differ in the symmetry of the induced waves on opposite sides of the source. The transition rate for an electric (magnetic) dipole depends on the electric (magnetic) mode density, i.e., the magnitude of the impedance. A transmission line resembles a magnetic dipole, but the fraction of the energy fed into the antenna is determined by impedance matching instead.[26−28] As a result, dipolar transitions dominantly excite different modes than the center-fed antennas usually considered in traditional antenna theory.

Resonant modes are expected for physical antenna lengths that are shifted from the multiples of π/k' by a constant value.[7,20,25] When the antenna is modeled as a cavity, this displacement can be introduced by a positive phase shift upon reflection[15,17,20] or by an extended cavity length.[25,26,29] The two corrections give the same resonant length but are otherwise not equivalent. We choose to set an extended length $L = L_p + L_c$ and a real-valued reflection coefficient r.

To derive the resultant current distribution $I(z,a)$ we do not distinguish between conduction and displacement currents and assume a one-dimensional (1D) sinusoidal distribution. A superposition in complex notation for time-harmonic waves gives, for $-L/2 \le z < a$

$$I(z,a) = \frac{I_0(e^{ika} \pm re^{ikL}e^{-ika})}{1 - r^2e^{2ikL}}(re^{ikL}e^{ikz} - e^{-ikz}) \qquad (2)$$

and for $a < z \le L/2$

$$I(z,a) = \frac{I_0(re^{ikL}e^{ika} \pm e^{-ika})}{1 - r^2e^{2ikL}}(e^{ikz} - re^{ikL}e^{-ikz}) \qquad (3)$$

The initial amplitude of the induced wave, I_0, depends on the type of dipole, its oscillator strength, and the three-dimensional (3D) configuration and modal fields.[23,29] Its value is not specified here, and because all the calculated rates are taken relative to other antenna lengths, none of the presented results depends on it.

The plus (+) signs in eq 2 and eq 3 are for electric dipoles and the minus (−) signs for magnetic dipoles; electric and magnetic dipoles couple effectively to the antenna modes at different positions, a result of the symmetry argument in Figure 1. The magnetic mode density maxima coincide with the electric mode density minima and vice versa.

The far field observed at r_0 is given by

$$E_\theta = E_0 \int_{-L/2}^{L/2} I(z,a)e^{-ik_\parallel z}\,dz \qquad (4)$$

in which $E_0 = i\eta_0 k_0 e^{ik_0 r_0} \sin\theta/(4\pi r_0)$ is the field of a point dipole at the origin, and $k_\parallel = k_0 \cos\theta$ is the parallel component of the wave vector $\mathbf{k_0}$ in the surrounding medium of impedance η_0. The other components of the electric field are zero. After evaluating the integral, eq 4 becomes

$$E_\theta = \frac{iI_0E_0}{1 - r^2e^{2ikL}}\left(A\left[\frac{re^{ikL}e^{-i(k_\parallel - k)z}}{k_\parallel - k} - \frac{e^{-i(k_\parallel + k)z}}{k_\parallel + k}\right]_{-L/2}^{a} + B\left[\frac{e^{-i(k_\parallel - k)z}}{k_\parallel - k} - \frac{re^{ikL}e^{-i(k_\parallel + k)z}}{k_\parallel + k}\right]_{a}^{L/2}\right) \qquad (5)$$

in which $A = e^{ika} \pm re^{ikL}e^{-ika}$ and $B = re^{ikL}e^{ika} \pm e^{-ika}$ contain the dependence on the dipole position.

The angular emission in eq 5 gives a complete description of the interaction of the antenna with a dipole and with radiation. The equation describes the emission of the dipole through the antenna mode and, by reciprocity,[9] its excitation by radiation. Indeed, by setting $r = 1$, which is equivalent to neglecting radiation damping, the results for the excitation of nanorods from Fabry−Pérot models[18,29] can be derived from eq 5 (see Supporting Information).

Next, we use the derived model to account for the radiation damping, study the main characteristics of optical antennas in a set of concrete examples, and compare the results to numerical simulations. We show in particular how the antenna characteristics evolve as the modes become increasingly more bound, i.e., plasmonic. As a measure of how bound antenna modes are, we define an effective index K

$$K \equiv k'/k_0 \qquad (6)$$

As a concrete case we choose cylindrical gold antennas with hemispherical ends, Figure 1a. The advantage of cylinders is that semianalytical waveguide solutions exist.[23] We study three radii, $R = 20$, 10 and 5 nm, which lead to three different values for K for the TM_0 modes.[23,25] The antenna length L is varied for a constant wavelength. As a source, we choose an electric dipole at the antenna end, because it effectively excites all relevant resonant modes. The dipole source in the 1D model is placed at the end of the extended cavity length: $a = -L/2$.

We first neglect the effect of the radiation damping on the current distribution by setting $r = 1$ and study the radiation damping by means of the radiation resistance, which we define as[26]

$$R_{rad} \equiv 2P/I_{max}^2 \qquad (7)$$

P is the total emitted power obtained by integrating the emitted far field given by eq 5, and I_{max} is the maximum of $|I(z)|$, eq 2 and eq 3. The radiation resistance gives the radiation damping per unit amplitude in the resonator; it is independent of the total amplitude and is a characteristic of the spatial distribution of the mode. After studying the radiation resistance, we will account for

dx.doi.org/10.1021/nl103828n |Nano Lett. XXXX, XXX, 000–000

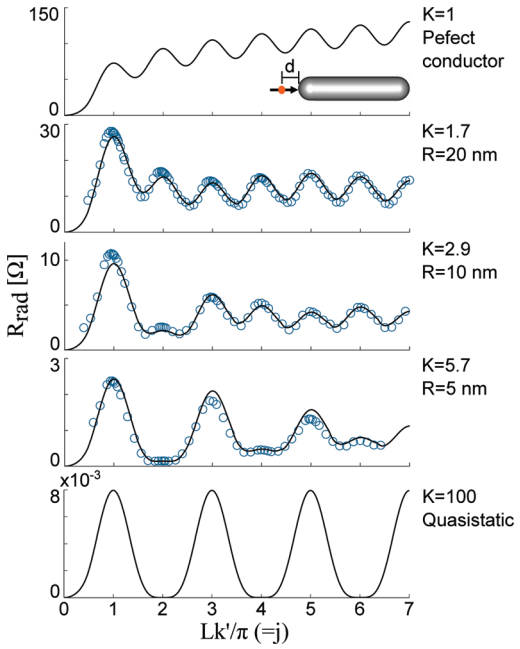

Figure 2. Evolution of the radiation resistance $R_{rad}(L)$ for increasingly bound antennas, i.e., increasing K. The optical antennas (K = 1.7, 2.9, and 5.7) are intermediate cases between the limits of perfect electrical conductors (K = 1) and quasi-statics ($K = 100 \gg 1$). Resonant modes occur if $Lk'/\pi = j$, with j an integer: lines, 1D model; circles, 3D Numerical calculations for cylindrical gold antennas in vacuum (CST MicroWave Studio, transient solver), Figure 1. **Parameters** λ_0 = 826.6 nm. *3D Numerical*: $\varepsilon_{au} = -29 + 2.0i$. Electric dipole at d = (5, 2.5, 1.25) nm for R = (20, 10, 5) nm, respectively (see inset). We used a hexahedral mesh, with a step size of (2, 1, 0.5) nm and a convergence criteria of −80 dB. *1D model*: Electric dipole at $a = -L/2$ and $r = 1$. For $K = 1$ and $K = 100$, $k'' = 0$. For R = 20, 10, and 5 nm: $k/k_0 = 1.7 + 0.045i$, $2.9 + 0.11i$, and $5.7 + 0.23i$, and L_c = 54, 26, and 12 nm.

the effect of the radiation damping on the amplitude of the mode by relating the reflection coefficient r to the radiation resistance.

The evolution of the radiation resistance with increasingly bound modes is illustrated in Figure 2, which shows R_{rad} as a function of L for the three optical antennas, together with the limiting cases of K = 1 (thin perfectly conducting antenna), and large K (quasi-static limit). We make the following three initial observations. First, the modes excited by electric dipoles at $a = -L/2$ differ from transmission-line center-fed antenna modes.[30] Magnetic dipoles at a = 0 do reproduce the results for center-fed perfectly conducting[30] (K = 1) and carbon nanotube[28] (K = 100) antennas. Second, unlike for K = 1, the radiation resistance for optical antennas does not increase with increasing length; the waves are bound. Third, the radiation resistance decreases with increasingly bound modes, i.e., increasing K.

In the quasi-static limit of $K \gg 1$, $K \propto 1/R$.[23] Equation 5 yields the scaling law $R_{rad} \propto 1/K^2$, which thus also implies $R_{rad} \propto R^2$. Furthermore, if one requires the resonances to depend only on the shape (or aspect ratio) of the antenna not on its absolute dimensions, then one must have $L_c \propto R$, or equivalently the reflection phase must be a constant, which gives a compelling argument supporting previous postulates,[25] and unexpected calculation results.[21,31]

We label the resonant modes j = 1, 2, ..., with $L = j\pi/k'$. Even and odd modes evolve differently. The radiation resistance of even modes diminishes with increasing K. These modes have

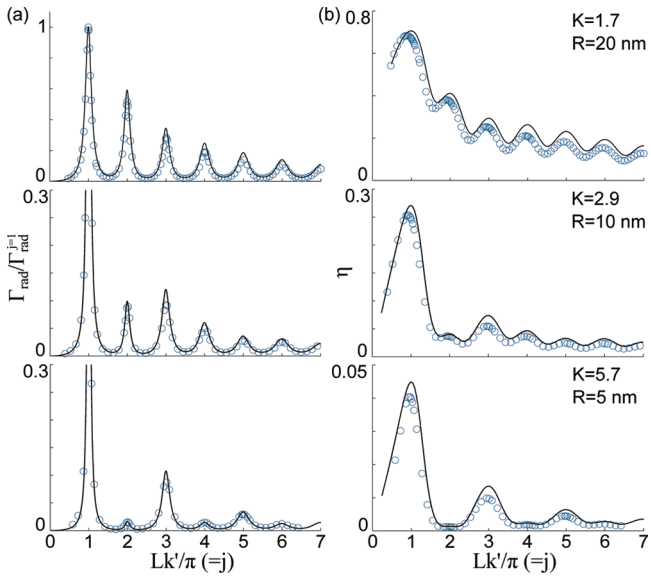

Figure 3. The radiative transition rate Γ_{rad} relative to the rate for j = 1 (a) and the quantum efficiency η (b) for the three optical antennas. All parameters as in Figure 2, but r from eq 8 with Z = 130.4, 219.4, and 414.8Ω.

antisymmetric current distributions and no net dipole moment.[32] For antennas shorter than half the free-space wavelength, such modes become subradient; opposite-oriented current elements cancel and the radiation resistance tends to zero. Odd modes behave oppositely and evolve into super-radiant modes with high radiation resistance. The criterium for super- and subradiance to manifest itself can be simply written as $K/j > 1$.

Because of super- and subradiance, the radiation damping clearly depends on the antenna length L; a nanorod is *not* a simple Fabry−Pérot cavity. Because the wave is bound, the radiation damping must be taken into account through the reflection coefficient r, which means that $r \neq 1$ and that r has to be a function of L. We relate r to the radiation resistance

$$r(L) = \frac{Z - R_{rad}/2}{Z + R_{rad}/2} \qquad (8)$$

in which Z is the real part of the antenna wave impedance and is determined from the waveguide solutions (i.e., considering an infinitely long rod) as: $Z = 2\int \mathbf{S}\cdot d\mathbf{A}/|\int \mathbf{J}\cdot d\mathbf{A}|^2$, in which $\mathbf{S}$ is the time-averaged Poynting vector, $\mathbf{J}$ is the current density, $d\mathbf{A}$ is oriented along the waveguide, and both integrals are over an infinite plane perpendicular to the waveguide. For $K \gg 1$, $Z \propto K$,[23] so that r approaches unity for large K (small radius R).

Equation 8 takes the form of an impedance matching equation and was obtained by equating the reflection loss in the cavity model with the radiation by the antenna. It relies on three arguments. First, all radiative loss is due to reflection, because the plasmon wave is bound. Second, the dissipation is small so that I_{max} is an approximate measure for the currents at all positions. Third, eq 8 introduces small deviations of r from unity, which can strongly affect the amplitude of the current distribution, but not the spatial distribution, so that the calculation of R_{rad} with r = 1 remains accurate.

With the radiation damping taken into account, the radiative transition rate Γ_{rad} ($\propto P$) can be compared quantitatively between the different resonant modes, Figure 3a. The relative

dx.doi.org/10.1021/nl103828n |*Nano Lett.* XXXX, XXX, 000–000

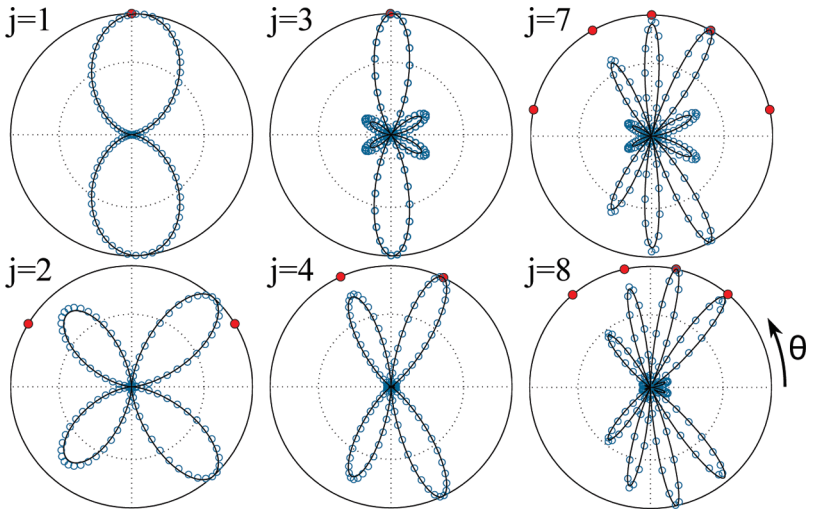

Figure 4. Angular (θ) emitted power for modes j: R = 20 nm (K = 1.7), all other parameters as in Figure 3; 1D model, line; 3D numerical, circles (blue); phase matching, eq 9, dots (red).

values for Γ_{rad} agree well with the numerical results. Without taking the radiation damping into account, no such agreement is obtained (see Supporting Information for a comparison).

Although for R = 20 all modes are pronounced, even modes disappear with increasing K. By reciprocity, a small Γ_{rad} also implies low field enhancements under far-field illumination;[9] these modes interact weakly with radiation and are dark modes.[33] Such dark modes combine subradiance, i.e., an antisymmetric current distribution (j = even) and a small antenna length ($K/j \gg 1$), with a significant dissipative loss that dominates the radiative loss. The analytical model presented here thus gives a quantitative description for the gradual emergence of such dark modes as antennas become increasingly plasmonic. Note that for larger K, higher order modes are in general weaker compared to the j = 1 mode; Γ_{rad} decays quicker with increasing L, because for lower R_{rad} the dissipative losses (k'', per unit length) gain in importance compared to the radiative losses (r, per reflection or round trip).

The balance between radiative and dissipative (Γ_{nr}) rates is described by the quantum efficiency $\eta = \Gamma_{rad}/(\Gamma_{rad} + \Gamma_{nr})$. Here, the intrinsic efficiency of the dipole emitter is taken as unity. The constant nonresonant dissipation due to the proximity of the dipole to the metal, i.e., due to coupling to lossy surface waves, is not included in the model and is subtracted from the numerical results. Thus, η is the antenna efficiency and sets an upper limit to the quantum efficiency of emission through the antenna modes.

The efficiency decreases with K, Figure 3b. Clearly, an efficient antenna should not be too plasmonic and should in general operate away from the quasi-static small-particle plasmon resonance. Because of the low radiation resistance of subradiant modes, the efficiency of even modes becomes particularly low and in this case even approaches zero, which explains why those modes become dark. Note that the local currents and fields are still resonantly enhanced (eq 2 and eq 3).[33] As a result large-K subradiant modes with low radiation damping, and consequently narrow line widths, can be advantageous in applications where efficient conversion into a photon is not required, or even unwanted. Examples are sensors[34] and spasers.[35]

The angular emission, eq 5, gives the angles under which the antenna emits and can be effectively excited. Unlike previous 0D models,[36] our model gives the emission patterns of higher order modes in good agreement with numerical calculations, Figure 4. Even modes do not interact with radiation perpendicular to the antenna axis, as expected by symmetry arguments.[13,18] Higher order modes can give multilobed patterns with an odd or even amount of maxima for odd or even modes, respectively. The patterns are obviously different from standard antenna theory (K = 1),[29,30] which yields j lobes, whereas optical antennas result in j or less lobes. The asymmetry in the patterns is caused by the radiative and dissipative losses and reveals the position of the dipole source.

We summarize the interaction of the resonant modes with radiation in a phase-matching equation for nanorods

$$k_{||} + (2m + 1)k_L = k' \qquad (9)$$

In which $k_L = \pi/L$, and m = 0, 1, 2, ..., approximately give the angles of maximum interaction, Figure 4.

The number of solutions for eq 9 determines the nature of the mode. Modes that do not give solutions for eq 9 are subradiant, do not interact effectively with radiation under any angle, and always emit as quadrupoles irrespective of the value of j. Modes with one solution are super-radiant, and always emit as dipoles. Modes with two or more solutions have multiple lobes and are neither subradiant nor super-radiant. Odd modes always give at least one solution, $m = (j - 1)/2$, whereas even modes only yield solutions if $Lk_0 > \pi$ (or $K/j < 1$). The number of solutions, and thus the angular emission, is determined by the antenna length, Lk_0, and the parity of the mode, not by the actual value of j. In other words, no direct information on the value of the mode number j propagates into the far-field, as is expected for a diffraction problem.

If $K \gg 1$, then $k_{||} \pm k \approx \pm k$, and the θ dependence of the denominator terms in eq 5 can be neglected. The emission is then a sum of three dipole terms: $E_0 e^{ik_{||}L/2}$, $E_0 e^{-ik_{||}L/2}$, and $E_0 e^{ik_{||}a}$, with the latter contribution negligible for strong modes. In this limit, the emission is thus described by two dipoles at the antenna ends, making a nanorod similar to a two-slit configuration, but with phases and amplitudes fixed by the plasmon wave. Equation 5 thus gives a mathematical basis for the commonly used intuitive picture of scattering of the mode at the antenna ends.[14,21,37,38]

The analytical results agree well with numerical calculations (Figure 2, Figure 3, and Figure 4). Only two fitting parameters

dx.doi.org/10.1021/nl103828n |Nano Lett. XXXX, XXX, 000–000

were used: k' and L_c. All other parameters were obtained from the waveguide solutions. The fitted values for k' differ by approximately 5% from the waveguide solutions, which is within the expected error margin of the numerical calculations. The fitted values for L_c are close to the previously used $2R$,[25] and follow the trends from previous calculations,[21,31] as well as the scaling laws derived here. For the specific configuration considered here, no good agreement is obtained if a phase shift, or an integration over only Lp, is used. The current distribution at the antenna ends is, in this case, better described by an additional length. However, a complete description of the ends is an open problem and a precise study of the problem is likely out of reach of the approximate 1D model presented here.

To conclude, the analytical model accurately describes the interaction of dipolar emitters with radiation through nanorod modes. The model includes radiation damping and is not limited to the quasi-static approximation, which is crucial because quasi-static antennas are usually inefficient antennas. The antenna properties are primarily governed by a single parameter, $K = k'/k_0$, that describes how plasmonic the antenna modes are and can be summarized in a phase-matching equation. Although here we focused on the evolution of the emission properties for increasingly bound waves, particularly the gradual emergence of sub-radiant, super-radiant and dark modes, the model applies to all interactions with any spatiotemporal beam and is equally valid for field enhancement and scattering problems. The results are thus widely applicable and might lead to further insights and design rules for optical antennas, nanorod spasers,[35] and generally for coupling light in/from nanorods.[13,14,20,21,37]

■ ASSOCIATED CONTENT

Supporting Information. Comparison of the present model with the models from Douillard et al.[18] and Dorfmuller et al.[29] This material is available free of charge via the Internet at http://pubs.acs.org/.

■ AUTHOR INFORMATION

Corresponding Author

*E-mail: Tim.Taminiau@icfo.es and Niek.vanHulst@icfo.es.

■ ACKNOWLEDGMENT

T.H.T. thanks R. Hildner, D. Brinks, A. G. Curto, R. Sapienza, R. Gordon, R. Zia, and C. I. Osorio for enjoyable discussions.

■ REFERENCES

(1) Greffet, J.-J. *Science* **2005**, *308*, 1561–1563.
(2) Taminiau, T. H.; Stefani, F. D.; Segerink, F. B.; van Hulst, N. F. *Nat. Photonics* **2008**, *2*, 234–237.
(3) Crozier, K. B.; Sundaramurthy, A.; Kino, G. S.; Quate, C. F. *J. Appl. Phys.* **2003**, *94*, 4632–4642.
(4) Muhlschlegel, P.; Eisler, H. J.; Martin, O. J. F.; Hecht, B.; Pohl, D. W. *Science* **2005**, *308*, 1607–1609.
(5) Kuhn, S.; Hakanson, U.; Rogobete, L.; Sandoghdar, V. *Phys. Rev. Lett.* **2006**, *97*, No. 017402.
(6) Anger, P.; Bharadwaj, P.; Novotny, L. *Phys. Rev. Lett.* **2006**, *96*, No. 113002.
(7) Taminiau, T. H.; Moerland, R. J.; Segerink, F. B.; Kuipers, L.; van Hulst, N. F. *Nano Lett.* **2007**, *7*, 28–33.
(8) Ringler, M.; Schwemer, A.; Wunderlich, M.; Nichtl, A.; Kurzinger, K.; Klar, T. A.; Feldmann, J. *Phys. Rev. Lett.* **2008**, *100*, 203002–4.
(9) Taminiau, T. H.; Stefani, F. D.; van Hulst, N. F. *Opt. Express* **2008**, *16*, 10858–10866.
(10) Curto, A. G.; Volpe, G.; Taminiau, T. H.; Kreuzer, M. P.; Quidant, R.; van Hulst, N. F. *Science* **2010**, *329*, 930–933.
(11) Asano, S.; Yamamoto, G. *Appl. Opt.* **1975**, *14*, 29–49.
(12) Bryant, G. W.; GarciadeAbajo, F. J.; Aizpurua, J. *Nano Lett.* **2008**, *8*, 631–636.
(13) Schider, G.; Krenn, J. R.; Hohenau, A.; Ditlbacher, H.; Leitner, A.; Aussenegg, F. R.; Schaich, W. L.; Puscasu, I.; Monacelli, B.; Boreman, G. *Phys. Rev. B* **2003**, *68*, No. 155427.
(14) Ditlbacher, H.; Hohenau, A.; Wagner, D.; Kreibig, U.; Rogers, M.; Hofer, F.; Aussenegg, F. R.; Krenn, J. R. *Phys. Rev. Lett.* **2005**, *95*, 257403–4.
(15) Della Valle, G.; Sondergaard, T.; Bozhevolnyi, S. I. *Opt. Express* **2008**, *16*, 6867–6876.
(16) Bozhevolnyi, S. I.; Sondergaard, T. *Opt. Express* **2007**, *15*, 10869–10877.
(17) Barnard, E. S.; White, J. S.; Chandran, A.; Brongersma, M. L. *Opt. Express* **2008**, *16*, 16529–16537.
(18) Douillard, L.; Charra, F.; Korczak, Z.; Bachelot, R.; Kostcheev, S.; Lerondel, G.; Adam, P.- M.; Royer, P. *Nano Lett.* **2008**, *8*, 935–940.
(19) Vesseur, E. J. R.; deWaele, R.; Kuttge, M.; Polman, A. *Nano Lett.* **2007**, *7*, 2843–2846.
(20) Dorfmuller, J.; Vogelgesang, R.; Weitz, R. T.; Rockstuhl, C.; Etrich, C.; Pertsch, T.; Lederer, F.; Kern, K. *Nano Lett.* **2009**, *9*, 2372–2377.
(21) Kolesov, R.; Grotz, B.; Balasubramanian, G.; Stohr, R. J.; Nicolet, A. A. L.; Hemmer, P. R.; Jelezko, F.; Wrachtrup, J. *Nat. Phys.* **2009**, *5*, 470–474.
(22) Li, Z.; Hao, F.; Huang, Y.; Fang, Y.; Nordlander, P.; Xu, H. *Nano Lett.* **2009**, *9*, 4383–4386.
(23) Chang, D. E.; Sorensen, A. S.; Hemmer, P. R.; Lukin, M. D. *Phys. Rev. B* **2007**, *76*, 035420–26.
(24) Encina, E. R.; Coronado, E. A. *J. Phys. Chem. C* **2007**, *111*, 16796–16801.
(25) Novotny, L. *Phys. Rev. Lett.* **2007**, *98*, No. 266802.
(26) Alu, A.; Engheta, N. *Phys. Rev. Lett.* **2008**, *101*, 043901–4.
(27) Alu, A.; Engheta, N. *Nat. Photonics* **2008**, *2*, 307–310.
(28) Burke, P. J.; Shengdong, L.; Zhen, Y. *IEEE Trans. Nanotechnol.* **2006**, *5*, 314–334.
(29) Dorfmuller, J.; Vogelgesang, R.; Khunsin, W.; Rockstuhl, C.; Etrich, C.; Kern, K. *Nano Lett.* **2010**, *10*, 3596–3603.
(30) Balanis, C. A. *Antenna Theory: Analyses and Design*, 3rd ed.; John Wiley and Sons, Inc.: Hoboken, NJ, 2005.
(31) Gordon, R. *Opt. Express* **2009**, *17*, 18621–18629.
(32) Aizpurua, J.; Bryant, G. W.; Richter, L. J.; Garcia de Abajo, F. J.; Kelley, B. K.; Mallouk, T. *Phys. Rev. B* **2005**, *71*, 235420–13.
(33) Liu, M.; Lee, T.-W.; Gray, S. K.; Guyot-Sionnest, P.; Pelton, M. *Phys. Rev. Lett.* **2009**, *102*, No. 107401.
(34) Hao, F.; Sonnefraud, Y.; Dorpe, P. V.; Maier, S. A.; Halas, N. J.; Nordlander, P. *Nano Lett.* **2008**, *8*, 3983–3988.
(35) Bergman, D. J.; Stockman, M. I. *Phys. Rev. Lett.* **2003**, *90*, No. 027402.
(36) Encina, E. R.; Coronado, E. A. *J. Phys. Chem. C* **2008**, *112*, 9586–9594.
(37) Akimov, A. V.; Mukherjee, A.; Yu, C. L.; Chang, D. E.; Zibrov, A. S.; Hemmer, P. R.; Park, H.; Lukin, M. D. *Nature* **2007**, *450*, 402–406.
(38) Ghenuche, P.; Cherukulappurath, S.; Taminiau, T. H.; van Hulst, N. F.; Quidant, R. *Phys. Rev. Lett.* **2008**, *101*, 116805–4.

dx.doi.org/10.1021/nl103828n |*Nano Lett.* XXXX, XXX, 000–000